Materials Physics and Mechanics 42 (2019) 609-616 Received: July 30, 2019

COMBINED EFFECT OF BORON ALLOYING AND AUSFORMING ON AUSTENITE TRANSFORMATION IN LOW CARBON STEELS UNDER CONTINUOUS COOLING

A.A. Vasilyev*, D.F. Sokolov, S.F. Sokolov, A.A. Zisman, N.G. Kolbasnikov

Peter the Great St. Petersburg Polytechnic University, Polytekhnicheskaya, 29

195251, St. Petersburg, Russia

*e-mail: vasilyev_aa@mail.ru

Abstract. The combined effect of boron addition and ausforming on the structure of low carbon low alloyed steel after the transformation of austenite has been investigated in a wide range of cooling rates. It is shown that boron hinders formation of polygonal ferrite in continuous cooling regardless of austenite predeformation and suppresses appearance of acicular ferrite. A qualitative explanation of this effect is proposed in terms of the deformation induced boron segregation on boundaries of austenite grains and subgrains. Practical significance of the obtained results is discussed in application to the thermomechanical treatment of the considered steels.

Keywords: steel, austenite transformation, deformation, boron, microstructure

1. Introduction

Boron still attracts attention of metal scientists [1-10] because even very low quantities (~ 10 ppm) of this relatively chip element hinders formation of ferrite and hence decreases temperatures of austenite transformation enabling fabrication of low carbon high strength steels with bainitic and martensitic structures at a moderate consumption of nickel, chromium and molybdenum. At the same time, owing to the higher moving force of the transformation at lower temperatures, the resulting structure becomes less sensitive to the parent austenite state that can somewhat devaluate efficiency of the thermomechanical treatment (TMT). This inevitable effect deserves special analysis since TMT of austenite is commonly used to refine the transformed structure in order to keep satisfactorily high fracture toughness of high strength steels. Meanwhile, although the problem has been addressed in several works [3,7], there are still no systematic data on the combined effect of boron and ausforming on transformed structures and properties of steels.

The present paper is aimed to investigate influence of microalloying by boron and ausforming on structures of low carbon low alloyed steel ($Cr + Ni + Mo < 0.6$ mass.%) obtained in a wide range of cooling rates. To implement various TMT and cooling conditions, thermomechanical simulator Gleeble 3800 (unit Pocket Jaw) has been employed.

2. Materials and experimental methods

Chemical compositions of investigated steels are represented in Table 1. Unlike steel S1 with an insignificant quantity of boron, its content in S2 should give an optimal effect on the transformed structure if this element is completely in the solid solution. To comply with the latter requirement, it is necessary to prevent formation of boron nitrides [11]; to this end, S2

http://dx.doi.org/10.18720/MPM.4252019_14

contains an appropriate quantity of titanium to immobilize all nitrogen in titanium nitrides. In terms of other alloying elements, the two steels differ insignificantly.

Table 1. Chemical compositions of the investigated steels (mass.%)

Steel	C	Mn	Si	Cr	Ni	Cu	Mo	Nb	V	Ti	N	B
S1	0.066	1.22	0.17	0.22	0.25	0.24	0.10	0.030	0.095	0.003	0.006	0.0003
S2	0.074	1.24	0.19	0.24	0.24	0.24	0.09	0.033	0.091	0.043	0.006	0.0025

Plates of 160×110×40 mm dimensions cut from laboratory ingots of both steels have been subjected to homogenization for 4 hrs at 1200°C, the following hot rolling (four passes) to the final thickness of 15 mm and air cooling. The employed heating mode before rolling is close to industrial regimes and ensures complete dissolution of Nb and V carbonitrides in the considered steels. To simulate TMT on unit Pocket Jaw of experimental complex Gleeble 3800, special specimens have been machined from the rolled plates. The following TMT regimes have been applied: reheating (5°C/s) to 1200°C, holding of 60 s, cooling (50°C/s) to 850°C; holding of 5 s (or compression with strain rate 1 s^{-1} to true strain $\varepsilon = 0.4$ and holding of 5 s); cooling with various rates (0.3, 1, 3, 10, 30 и 100°C/s) to room temperature.

Making use of program Thermo-Calc [12], the deformation temperature (850°C) has been selected to exceed by not less than 30 °C the temperature of phase paraequilibrium that is 820 and 816°C for steels S1 and S2, respectively. Such a selection excludes the austenite transformation start during ausforming; this conclusion has been eventually confirmed by dilatometric data recorded in terms of diameter changing in the specimen work part. Such data are also used to obtain the temperature dependence of the transformation degree; 1 and 99% of the latter then have been associated with characteristic temperatures A_{r3} and A_{r1}.

Polished sections of specimens have been etched in reagent Nital at room temperature and their microstructures then have been investigated on optical microscope Axio Observer «Carl Zeiss» equipped with automated system Thixomet for image analysis. In addition to usual metallographic microstructures, this system enabled us to get average sizes of prior austenite grains which proved to be 60 and 54 μm for S1 and S2, respectively. Hardness (HV10) for each microstructure has been determined with installment Zwick/Roell by averaging of five measurements.

2. Results

Under consideration are the following structure components of the investigated steels: polygonal ferrite (PF), allotriomorphic ferrite (ALF), perlite (P), granular bainite (GB), lath bainite (LB) often cited as bainitic ferrite, and specific deformation-induced bainite currently called acicular ferrite [13]. For brevity sake, we will show results only for four cooling rates (0.3, 3, 10 и 30°C/s) from six that is enough to reveal the main regularities which would not change with allowance for the omitted data. Microstructures obtained with no ausforming ($\varepsilon = 0$) and with the true starin $\varepsilon = 0.4$ of austenite are shown in Fig. 1 and 2, respectively.

Let us consider the case of $\varepsilon = 0$ first. Then, after the slowest cooling (0.3°C/s), the microstructure of steel S1 consists mainly of PF with small additions of GB and P (Fig. 1a). When the cooling rate increases, various types of bainitic microstructures appear (Fig. 1c, e, g). Note that some amounts of ferrite are saved in this steel up to the highest cooling rate 30 °C/s (Fig. 1g). Thus, at 3°C/s there exists a distinct fraction of PF (Fig. 1c) whereas at higher cooling rates some amount of ALF appears that can be revealed with an appropriate magnification (Fig. 1g).

No PF is revealed in steel S2 without ausforming even at the least cooling rate (Fig. 1b) and only bainitic microstructures appear at all cooling rates. When comparing the same rates, the fraction of LB in S2 is always higher than in S1 (Fig. 1c–h). It is worth noting that after the quick cooling (30°C/s) boundaries of prior austenite grains (PAGB), where bainite laths form (Fig. 1h), are easy to reveal on the background of LB only in steel S2; in steel S1 imaging of PAGB after the same cooling rate becomes less reliable (Fig. 1g). This property of S1 is due to formation of ALF that partly consumes PAGB.

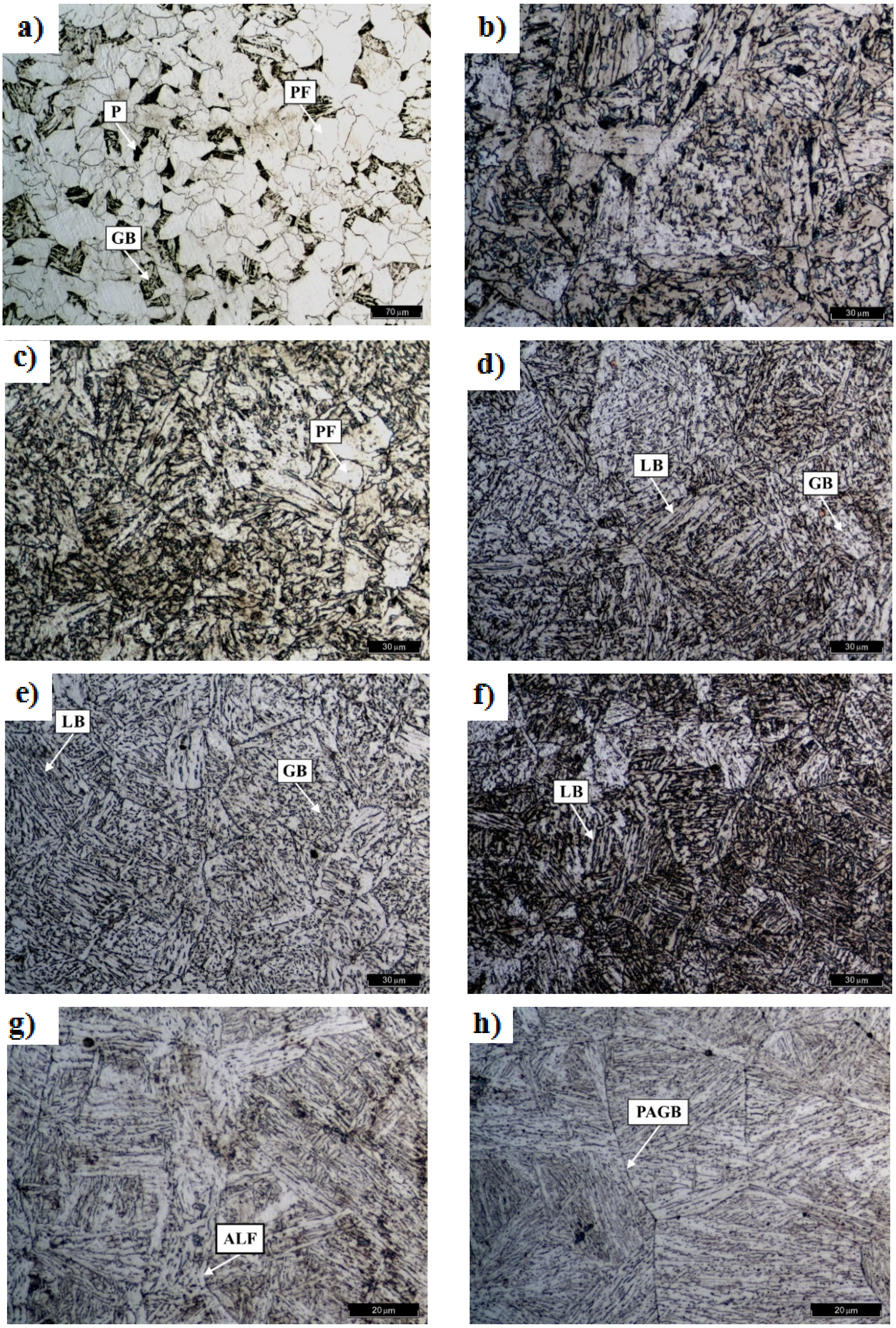

Fig. 1. Microstructures of steels S1 (left) and S2 (right) obtained at ε = 0 and cooling rates 0.3 (a,b), 3 (c,d), 10 (e,f) and 30 °C/s (g,h)

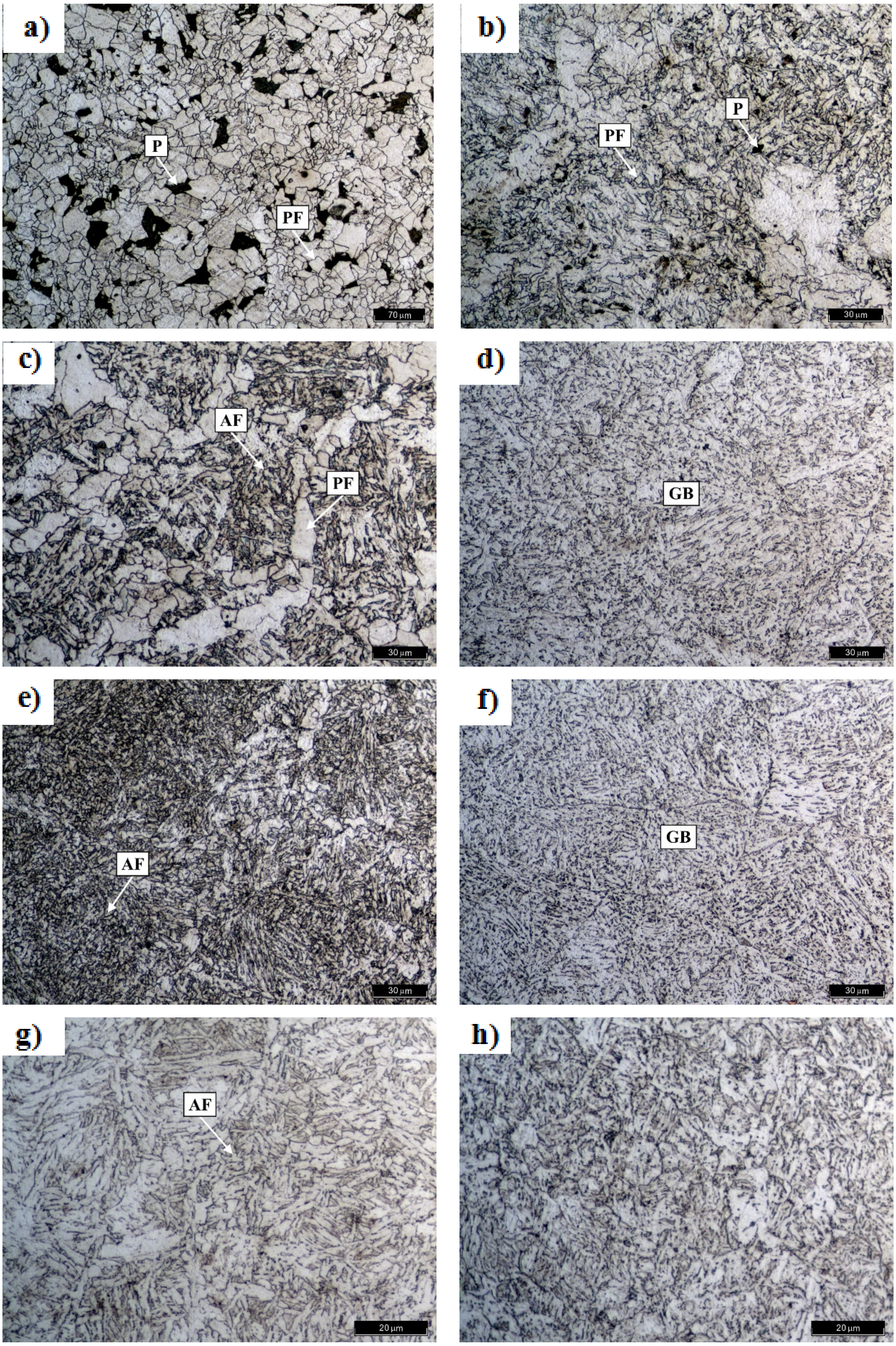

Fig. 2. Microstructures of steels S1 (left) and S2 (right) obtained at $\varepsilon = 0.4$ and cooling rates 0.3 (a,b), 3 (c,d), 10 (e,f) and 30 °C/s (g,h)

The above-considered difference between microstructures of S1 and S2 comply with respective dependences of temperatures A_{r3} and A_{r1} on cooling rates, as evident in Fig. 3a.

Thus, at low rates A_{r3} is notably higher for S1; at rates exceeding 10 °C/s this effect weakens, yet the whole temperature range of S2 transformation is still situated notably lower. Accordingly, microstructures of S2 has higher hardness after all cooling rates, Fig. 4.

Next, let us consider microstructures obtained with ausforming ($\varepsilon = 0.4$). Austenite transformation in S1 at the least cooling rate forms a ferritic-pearlitic microstructure where dimensions of PF grains are notably less than in case of $\varepsilon = 0$ (Fig. 1a and 2a). This corresponds to the known effect of accelerated ferrite formation in transformation of the deformed austenite. When the cooling rate grows, AF gradually appears and its fraction becomes very distinct at 10 и 30 °C/s (Fig. 2e, g). Unlike steel S1, bainitic constituents predominates in S2 even at the least cooling rate where only minor fractions of P and small PF grains can be found, Fig. 2b. At higher rates there is no PF. Another important distinction of S2 is an almost complete absence of AF; at all cooling rates higher than 3 °C/s mostly GB is formed (Fig. 2d, f, h).

As evident in Fig. 3b, the transformation of deformed austenite in S2 takes place in notably lower temperatures than in S1. At all cooling rates, except for 10 °C/c, the corresponding difference in hardness proves to be much higher than in case of $\varepsilon = 0$, Fig. 4.

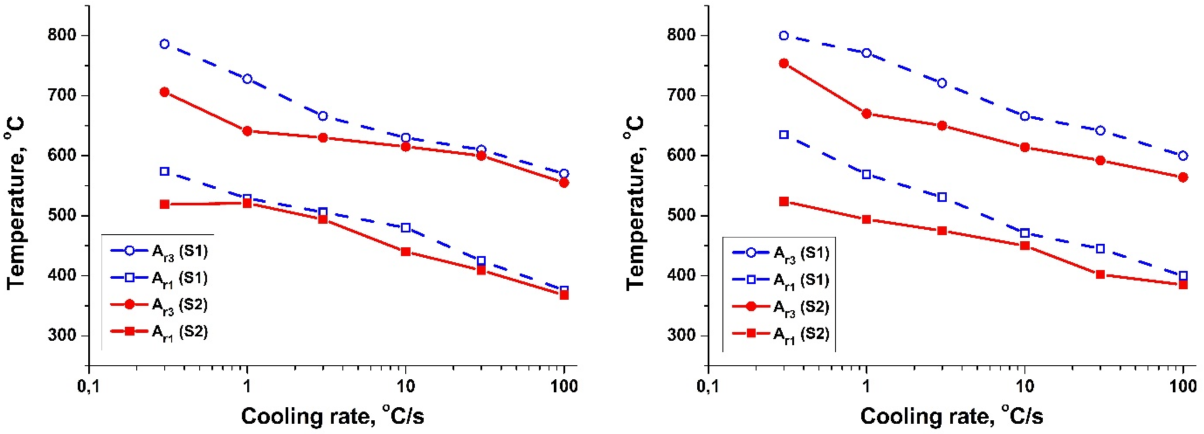

a) **b)**

Fig. 3. Dependences of temperatures A_{r3} and A_{r1} on cooling rate of steels S1and S2 with undeformed (a) and deformed (b) austenite

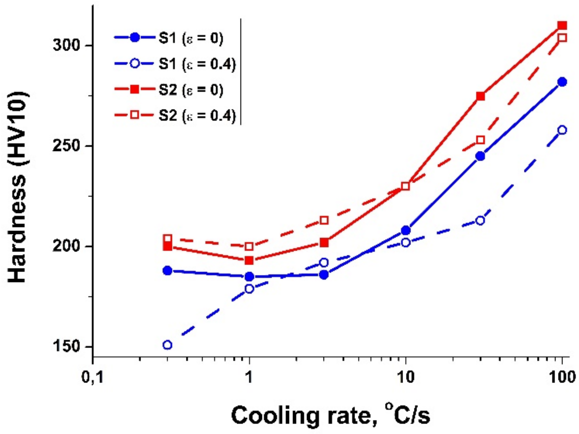

Fig. 4. Dependences of hardness (HV10) of obtained structures on cooling rate for steels S1 and S2 at $\varepsilon = 0; 0.4$

3. Discussion

To sum up obtained experimental results, microalloying by boron provides a notable effect on microstructures formed in a wide range of cooling rates (5 to 30°C/s) of *predeformed* austenite. Specifically, morphologically similar microstructures with the most GB fraction and gradually changing hardness are observed. In other words, the combined effect of boron and ausforming is hopefully a means to enable the through-thickness hardenability of large semiproducts of high strength steels that would be of great practical significance. To evaluate the above-mentioned perspectives, however, mechanical properties of the considered microstructures, particularly ductility and fracture toughness, should be properly investigated. Indeed, unlike conventional chemical compositions where TMT of γ–phase at appropriately low temperatures notably refines structures of the eventual α–phase, boron microalloying suppresses this effect and hence necessitates alternative approaches to the structure refinement. For instance, this may be achieved in the rough (higher temperature) stages of hot rolling by the repeated static recrystallization of austenite in pauses between successive deformations [14].

Apart from the known effect of boron on the transformation of *undeformed* austenite (predominance of shear modes, i.e. suppression of PF and ALF), the obtained results indicate specific regularities of boron influence in case of previous ausforming as follows. It has been shown first that boron hinders formation of ferrite even after significant predeformation of austenite. Moreover, despite the latter, boron suppresses formation of AF at in-grain features of deformation substructure; this effect is particularly notable as far as AF is a kind of bainite, i.e. a product of shear transformation [13].

In order to analyze the underlying mechanisms in a more formal way, it is expedient to consider diffusion of boron in austenite before its deformation. According to [15], atoms of this element in γ–phase of steel can occupy both substitution and interstitial positions and, hence, the two respective modes of diffusivity can take place. Corresponding estimates [16,17] show that the average diffusion path of boron during 7 s of cooling from 1200°C to 850°C (deformation temperature) is 20 or 50 µm in case of substitution or interstitial diffusivity, respectively. With the PAG size of about 54 µm, this means that boron atoms always have enough time to segregate at PAGB and at their surroundings [18] before the deformation followed by cooling. Such estimates also comply with a usual boron effect (suppression of all ferrite types) in the transformation of undeformed austenite.

To understand disappearance of PF and ALF owing to the boron addition, let us consider first accelerated formation of such phases at PAGB of deformed austenite in boron-free steels [19,20]. This effect is due to hydrostatic tensile stresses [22] generated by defects induced by deformation at some PAGB junctions. These stresses compensate compressive stresses, arising in constraint of nascent phase (ferrite) with a higher specific volume, and hence increase a driving force of the transformation. On the other hand, in steel S2 the deformation-induced elastic fields result in diffusion of boron atoms to such junctions and thus reduce the previously mentioned deformation effect. When compared to the substitutional mechanism assisted by vacancies, diffusion of boron interstitials, producing strong elastic distortions of austenite lattice [23], is certainly more efficient from the considered viewpoint. However, both mechanisms are kinetically possible since the related diffusion paths are long enough. Thus, for example, during the cooling from 850 to 775°C at cooling rate of 1°C/s (Fig. 3b) these paths are 15 and 50 µm for the boron substitutions and interstitials, respectively.

Suppression of AF that is a deformation-induced kind of bainite is the least expected effect of boron revealed in the present study. According to the conventional viewpoint, the dislocation substructure of austenite hinders the *growth* of bainitic embryos and thus results in a complicated mixture of small transformed crystals. However, this work provides some evidence for the boron effect on the displacive rearrangement of atoms in the bainite *nucleation*. Indeed, facilitated penetration of transformed crystals through the substructure of austenite, i.e. no AF suggests a higher driving force (overcooling) at the transformation start. Further investigations are needful to clear up this issue. In any case, the above-mentioned diffusion paths of boron are sufficient to form segregation of this element in austenite at PAGB or their surroundings and, moreover, at dislocation boundaries. Besides, formation of the latter and hence of the austenite substructure, responsible for AF, can be somewhat retarded owing to the boron atmospheres at dislocations.

4. Conclusions

It is shown that microalloying of low carbon steel by boron suppresses formation of PF in continuous cooling regardless of the austenite predeformation. Besides, what is rather surprising, boron also prevents formation of AF. Consequently, the transformation of austenite in a wide range of cooling rates produces in boron-microalloyed steel uniform morphologically similar microstructures with the predominant fraction of GB and high hardness. At the same time, these results necessitate certain reconsideration of TMT technologies. Unlike conventional chemical compositions, where TMT leads to notable refinement of the transformed structure, this favorable effect is essentially reduced by boron. Thus, to keep high fracture toughness of steel in this case, other approaches to the structure refinement should be employed. In particular, a possible means is to make use of repeated static recrystallization of austenite in pauses between successive deformations in the fractional hot rolling.

Acknowledgments. *This work was supported by the grant from the Russian Science Foundation (project No. 19-19-00281).*

References

[1] Wang XM, He XL. Effect of boron on copper induced surface hot shortness of 0.1% carbon steel. *Iron and Steel Institute of Japan International*. 2002;42: S38-S46.

[2] Hara T, Asahi H, Uemori R, Tamehiro H. Role of combined addition of niobium and boron and of molybdenum and boron on hardenability in low carbon steels. *Iron and Steel Institute of Japan International*. 2004;44(8): 1431-1440.

[3] Jun HJ, Kang JS, Seo DH, Kang KB, Park CG. Effects of deformation and boron on microstructure and continuous cooling transformation in low carbon HSLA steels. *Materials Science and Engineering: A*. 2006;422(1-2): 157-162.

[4] Khare S, Lee K, Bhadeshia H.K.D.H. Relative effects of Mo and B on ferrite and bainite kinetics in strong steels. *International Journal of Materials Research.* 2009;100(11): 1513-1520.

[5] Zhu K, Oberbilling C, Music C, Loison D, Iung T. Effect of B and B + Nb on the bainitic transformation in low carbon steels. *Materials Science and Engineering: A*. 2011;528(12): 4222-4231.

[6] Hwang B, Suh DW, Kim SJ. Austenitizing temperature and hardenability of low-carbon boron steels. *Scripta Materialia*. 2011;64(12): 1118-1120.

[7] Deva A, Jha N, Jha B. Effect of austenitizing temperature and cooling condition on mechanical properties of low carbon boron containing steel. *International Journal of Metallurgical Engineering*. 2012;1(1): 1-6.

[8] Mun DJ, Shin EJ, Choi YW, Lee JS, Koo YM. Effects of cooling rate, austenitizing temperature and austenite deformation on the transformation behavior of high-strength boron steel. *Materials Science and Engineering: A*. 2012;545: 214-224.

[9] Terzic A, Calcagnotto M, Guk S, Schulz T, Kawalla R. Influence of boron on transformation behavior during continuous cooling of low alloyed steels. *Materials Science and Engineering: A*. 2013;584(1): 32-40.

[10] Song T, De Cooman BC. Effect of boron on the isothermal bainite transformation. *Metallurgical and Materials Transactions A*. 2013;44(4): 1686-1705.

[11] Lin HR, Cheng GH. Hardenability effect of boron on carbon steels. *Materials Science and Technology*. 1987;3(10): 855-859.

[12] *Thermo-Calc Software*. Available from: http://www.thermocalc.com [accessed 26th November 2019].

[13] Zhao H, Wynne BP, Palmiere EJ. Conditions for the occurrence of acicular ferrite transformation in HSLA steels. *Journal of Materials Science. Metals*. 2018;53(5): 3785-3804.

[14] Soshina TV, Zisman AA, Hlusova EI. Revealing prior austenite grains and analysis of the metadynamic recrystallization kinetics of austenite in low carbon steel. *Letters on Materials*. 2012;2(1): 3-8.

[15] McLellan RB, Ko C. The diffusion of boron in f.c.c. iron. *Journal of Physics and Chemistry of Solids*. 1993;54(4): 465-468.

[16] Zhang X, Li X, Wu P, Chen S, Zhang S, Chen N, Huai X. First principles calculation of boron diffusion in fcc-Fe. *Current Applied Physics*. 2018;18(10): 1108-1112.

[17] Li X, Wu P, Zhao S, Chen C, Yin R, Chen N. First-principle study of the solution type of boron in γ-iron. *Energy Procedia*. 2012;16: 661-666.

[18] Karlsson L. Overview no. 63 Non-equilibrium grain boundary segregation of boron in austenitic stainless steel − III. Computer simulations. *Acta Metallurgica*. 1988;36(1): 25-34.

[19] Inagaki H. Effect of controlled rolling on the ferrite-pearlite transformation in a low-carbon Nb steel. *Zeitschrift für Metallkunde*. 1986;77(1): 36-42.

[20] Hanlon DN, Sietsma J, van der Zwaag S. The effect of plastic deformation of austenite on the kinetics of subsequent ferrite formation. *Iron and Steel Institute of Japan International*. 2001;41(9): 1028-1036.

[21] Sokolov DF, Ogoltcov AA, Vasilyev AA, Kolbasnikov NG, Sokolov SF. Modeling of microstructure and mechanical properties of hot rolled steels. *Materials Science Forum*. 2013;762: 116-121.

[22] Zisman AA, Rybin VV. Mesoscopic stress field arising from the grain interaction in plastically deformed polycrystals. *Acta Materialia*. 1998;46(2): 457-464.

[23] Kraposhin VS, Talis AL, Kamenskaya NI, Arestov V, Zaitsev AI. Arrangement of collective B12 atoms in the crystal structure of γ-Fe and effect of boron on the hardenability of steel. *Metal Science and Heat Treatment*. 2018;60(1-2): 63-71.